*Aerosol and Air Quality Research*, 17: 1256–1266, 2017

ISSN: 1680-8584 print / 2071-1409 online
doi: 10.4209/aaqr.2016.11.0500

# Measurement and Evaluation of Elastic Light Scattering from a Single Levitated Irregular Particle

**Yuan-Yi Kao[1], Sheng-Hsiu Huang[2], Chih-Chieh Chen[2], Cheng-Shiun Tsai[1], Chang-Huei Wu[3], Wen-Yinn Lin[1*]**

[1] *Institute of Environmental Engineering and Management, National Taipei University of Technology, Taipei 10608, Taiwan*
[2] *Institute of Occupational Medicine and Industrial Hygiene, National Taiwan University, Taipei 10055, Taiwan*
[3] *Department of Mechanical Engineering, Yuan Ze University, Taoyuan 320, Taiwan*

## ABSTRACT

This study introduced a convenient experimental method to measure and to evaluate the elastic light scattering from a single irregular particle. The particle levitation system was used to trap a particle and to maintain the particle at null position by utilizing electrodynamic balance. Moreover, the Raman spectroscopy was applied to observe the light scattering of a single particle. The influences of relative humidity on optical properties of particle were also discussed. For comparison with experimental results, the classical Lorenz-Mie theory was employed to compute the phase function of a single particle. The experimental results demonstrated that the measurements of light scattering were in approximate trend with the model. In particular, numerical simulation results showed that the scattering intensity was underestimated in backward scattering directions. Consequently, the effect of surface roughness and irregular morphology of particle might be resulted in deviations of backward scattering. Besides, the experiments suggested that while using the weighted average method to estimate the refractive index might cause some significant deviations of light scattering between measuring and modeling.

***Keywords:*** Irregular particle; Light scattering; Electrodynamic balance; Levitation.

## INTRODUCTION

Within the last few decades, scattering and absorption light of spherical particle which affect solar radiative forcing and/or visibility had been widely studied and were well understood (Charlson *et al.*, 1992; Kiehl and Briegleb, 1993; Lee and Hsu, 1999; Chen *et al.*, 2000; Friedlander, 2000; Lin *et al.*, 2000; Watson *et al.*, 2005; Lin *et al.*, 2009; Lin *et al.*, 2010; Wu *et al.*, 2012; IPCC, 2013; Kim, 2015; Pu *et al.*, 2015; Fukushima *et al.*, 2016; Molnár *et al.*, 2016). Though, light scattering or light absorption from irregular or non-spherical particle perseveres with a paradox. There were many types of this particle such as dust, mineral and soot aerosol, volcanic ash, snow crystal, and biological spore, etc. which could find in different environments. Further, the effects of irregular or non-spherical particle on electromagnetic scattering and remote-sensing recoveries had been extensively discussed in recent times (Volten *et al.*, 1996; Li *et al.*, 2004; Moreno *et al.*, 2006; Liu and Mishchenko, 2007; Muñoz *et al.*, 2010; Muñoz and Hovenier, 2011; Petrov *et al.*, 2011; Hajihashemi and Jiang, 2013; Zubko *et al.*, 2013; Bagheri *et al.*, 2015; Milstein and Richardson, 2015; Wang *et al.*, 2015; Yang *et al.*, 2015). The size, shape, and surface texture characterization play an influential role in establishing the optical properties of the irregular or non-spherical particle which was often associated with many uncertainties. To neglect the nonsphericity of particle may cause a significant underestimation or overestimation of light scattering (Li *et al.*, 2004; Yang *et al.*, 2007).

Modeling of light scattering from particle also plays an important role in determining optical characterization of aerosol. The Lorenz-Mie theory was a classical method to calculate the scattering properties of a single homogeneous particle. It was not only used to calculate scattering and absorption cross-sections but also the angular scattering for diameter of spherical particle, refractive index, and wavelength of incident light (De Leeuw and Lamberts, 1987; Ma, 2007; Li *et al.*, 2012; Dlugach and Mishchenko, 2014; Han *et al.*, 2014; Greengard *et al.*, 2015; Briard *et al.*, 2016). The phase function was dependent on the refractive index, the incident wavelength, and the particle size. Accordingly, the phase function could be utilized to calculate the particle diameter (Chang and Biswas, 1992; Gatherer *et al.*, 2002; Hopkins *et al.*, 2003; Mitchem *et al.*, 2006; Symes *et al.*, 2006; Davies *et al.*, 2012; Haddrell *et al.*, 2013). In

* Corresponding author.
Tel.: +886-2-27712171 ext. 4131; Fax: +886-2-27781598
*E-mail address:* wylin@ntut.edu.tw

addition, the chemical composition or mixing state of particle could influence the refractive index, size, and density, which in sequence directly affect their optical properties (Liu and Mishchenko, 2007; Gangl *et al.*, 2008).

In order to recognize optical properties of particle, systematic measurements may first be accomplished on a single levitation particle under laboratory conditions. Investigation of single particle studies started in the early part of the twentieth century by using Millikan condenser to measure the elementary charge on the electron. Basing on the oil droplet experiment, the electrodynamic balance (EDB) had been used to capture and levitate a single particle in an electric field. Through this original study, many investigations as well as physical and chemical properties of single particle had been measured and demonstrated by utilizing different kinds of levitating technique such as electrostatic trapping, acoustic balance, and optical levitation (Millikan, 1935; Richardson *et al.*, 1989; Davis and Bridges, 1994; Davis, 1997; Peng and Chan, 2001; Haddrell *et al.*, 2005; Jarzembski and Tankosic, 2005; Mitchem *et al.*, 2006; Nakajima, 2006; Tsai, 2007; Chan and Chan, 2007; Kelly *et al.*, 2008; Kawamoto, 2009; Reid, 2009; Wills *et al.*, 2009; Knox *et al.*, 2010; Zaitone and Tropea, 2011; Davies *et al.*, 2012; Haddrell *et al.*, 2014).

Although many studies had discussed the optical characterization of irregular or non-spherical particle by using numerical simulation, few had been carried out on the determination by using experimental method. Hence, this study devised an automatic and useful experimental method; moreover, the comparison with the Lorenz-Mie theory model that could obtain the scattering function of a single irregular particle as well as capture optical properties related to particle size and refractive index.

## MATERIALS AND METHODS

The experiments and simulations, described as following sections, experimental apparatus included three major systems, i.e., the automatically controlled electrodynamic balance (EDB) system, the charge coupled device (CCD) camera monitoring system, and the particle scattering measurement system. The specifications of refractive index for each test Polymethyl methacrylate (PMMA) and carbon particles were 1.49 and 2-i, respectively (Cariou *et al.*, 1986; Hinds, 1999).

### *Simulation of Mie Scattering*

In the following, a brief overview of the equations which were used in this study was given. The Mie scattering properties were computed by using the scattering amplitude functions $i_1$ and $i_2$, which described the scattering at a particular angle with polarization perpendicular and parallel to the scattering plane, respectively. To consider a spherical particle falling into Mie size range that was illuminated with polarized light of intensity, the amplitude functions could be defined as following equations:

$$i_1(\mu) = \sum_{k=1}^{\infty} \frac{2k+1}{k(k+1)} \left[ a_k \pi_k(\mu) + b_k \tau_k(\mu) \right] \quad (1)$$

$$i_2(\mu) = \sum_{k=1}^{\infty} \frac{2k+1}{k(k+1)} \left[ a_k \tau_k(\mu) + b_k \pi_k(\mu) \right] \quad (2)$$

where $\mu = \cos\theta_{scat}$, $a_k$ and $b_k$ were the Mie scattering coefficients and the functions $\pi_k(\mu)$ and $\tau_k(\mu)$ contained the information about angular dependence. This numerical solution of the Mie regime particle was restricted to the size parameter regime $\leq 10^4$–$10^5$ (van de Hulst, 1981; Shah, 1992). Besides, the $\theta$ was the angle between the direction of the incident light and the scattered radiation. The angular functions $\pi_k(\mu)$ and $\tau_k(\mu)$ could be defined as the simple recursive relations :

$$\pi_{k+2} = \frac{2k+3}{k+1} \mu \pi_{k+1} - \frac{k+2}{k+1} \pi_k \quad (3)$$

$$\tau_{k+2} = (k+2)\mu\pi_{k+2} - (k+3)\,\pi_{k+1} \quad (4)$$

starting from $\pi_0 = 0$ and $\pi_1 = 1$.

The Mie coefficients $a_k$ and $b_k$ were defined as following functions:

$$a_k = \frac{\psi_k'(mx)\psi_k(x) - m\psi_k(mx)\psi_k'(x)}{\psi_k'(mx)\zeta_k(x) - m\psi_k(mx)\zeta_k'(x)} \quad (5)$$

$$b_k = \frac{m\psi_k'(mx)\psi_k(x) - \psi_k(mx)\psi_k'(x)}{m\psi_k'(mx)\zeta_k(x) - \psi_k(mx)\zeta_k'(x)} \quad (6)$$

Their numerical evaluations and the more detailed descriptions could be found in standard references in Lorenz-Mie theory (van de Hulst, 1981; Bohren and Huffman, 1983; Davis and Schweiger, 2002; Wolfram and Thomas, 2012). Additionally, the subroutine DAMIE was used to calculate the scattering cross section of PMMA and carbon particle (Dave, 1968).

### *Automatically Controlled Electrodynamic Balance System*

As shown in Fig. 1, an auto-controlled EDB system was used in this study. The factors of the custom-built EDB cell were shown in Table 1. The particle was illuminated with a 30 mW solid-laser ($\lambda$ = 532 nm) and imaged on a monitor with a CCD camera using a zoom lens, so the particle's location upon entering the null position of the balance was monitored.

The EDB was combined alternating current (AC) electric fields with direct current (DC) electric fields in order to capture and levitate a single charged particle at the null position of the electric field. Because of the dry dispersion method used, the particles would ordinarily carry out one or more excess electrons through contact charging. The levitated particle was stabilized by charging of the alternating electric field ($V_{ac}$), specifically the amplitude and frequency of the central double-ring electrodes. Assuming that there was no loss of particle's charge, the mass of the particle was proportional to the inputted DC voltage ($V_{dc}$). By employing

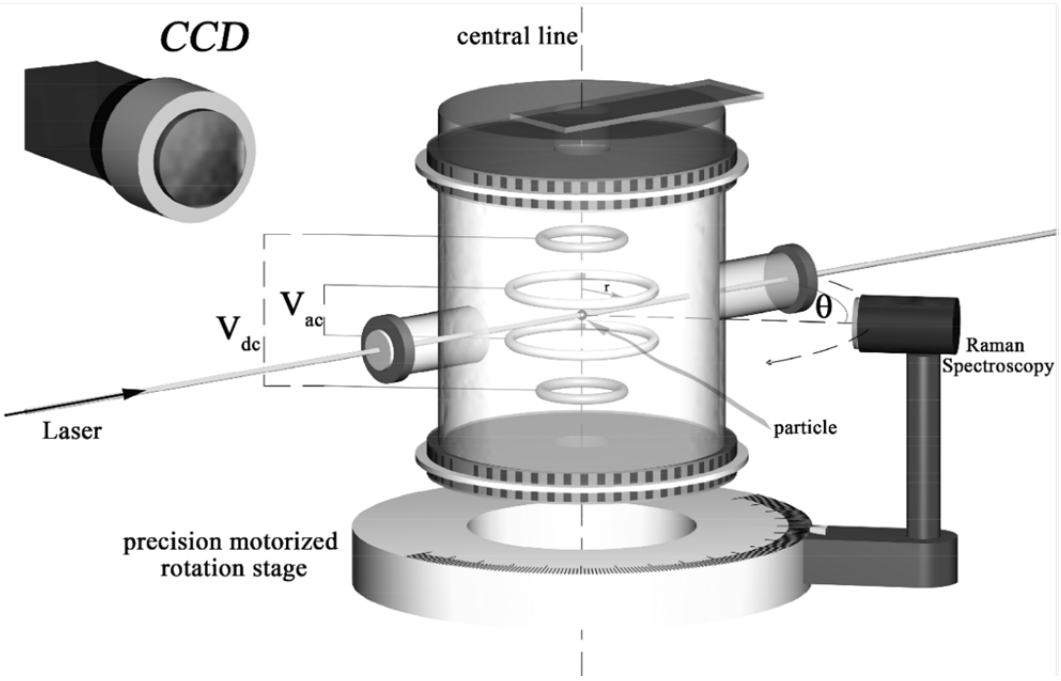


**Fig. 1.** Schematic of the automatically electrodynamic balance system.

**Table 1.** The factors of the custom-built EDB cell.

| Item | Unit |
|---|---|
| DC electrode | 12 mm in diameter |
| AC electrode | 16 mm in diameter |
| The distance between upper and lower electrode ($V_{dc}$) | 20 mm |
| The distance between central double-ring electrodes ($V_{ac}$) | 10 mm |
| The voltage of alternating current ($V_{ac}$) | < 2000V, 1 mA |
| The frequency of the $V_{ac}$ | 0.3 Hz–3 MHz |

the LabVIEW software, the position of levitated particle on the display provided system with feedback signal to adjust the $V_{dc}$ for saving particle at null position automatically.

A $V_{ac}$ was applied to the central double-ring electrodes, coming about a null potential at the geometric center of the alternating electric field. The alternating current potential of the balance was defined as following equation:

$$V_{ac} = \frac{V(t)}{\cos \Omega t} \times \theta \left( \frac{Z_0^2}{Z^2 - \frac{r^2}{2}} \right) \tag{7}$$

where $\Omega = 2\pi f$ was angular frequency of the alternating potential and r was radius of the central double-ring electrodes.

A $V_{dc}$ was applied to upper and lower ring electrode to balance a charged particle with the gravitational force in the null position. Thus, the direct current potential was defined as following equation:

$$V_{dc} = \frac{gZ_0}{C_0} \times \frac{m}{nq} \tag{8}$$

where $C_0$ was a geometric factor, g was the acceleration of gravity, m was the mass of the particle, $Z_0$ was the separation distance of the upper and lower ring electrode, n was the number of elementary charges present on the particle, and q was the elementary charge (Davis, 1985; Jarzembski and Tankosic, 2005).

***Light Scattering of Single Levitated Particles***

The EDB cell was combined with a precision motorized rotation stage and these two devices were positioned at the same central line. This stage could rotate continuously through a full 360 degrees, and furthermore the range from 40 to 140 degrees was utilized in the experiment. Therefore, there had some restrictions on the measurement of the light scattering behavior that predominantly scattered forward or backward, it had to design another system which collects light by means of a fixed lens. The Raman spectroscopy (model QE65000, Ocean Optics, USA) was introduced to measure the scattering of the levitated particles undergoing experimental conditions. The specifications of the Raman spectroscopy were categorized in Table 2. In general, Raman spectroscopy provides information about molecular vibrations that could be used for identification or quantitation of particle's components. Nevertheless, it was utilized to

**Table 2.** The specifications of the commercial Raman spectroscopy.

| Physical | |
|---|---|
| Dimensions | 182 × 110 × 47 mm |
| Weight | 1.18 kg (without power supply) |
| Detector | |
| Detector model | Hamamatsu S7031-1006 |
| Detector range | 200–1100 nm |
| Pixels | 1024 × 58 |
| Pixel size | 24 $\mu m^2$ |
| Pixel well depth | 1000 Ke- |
| Sensitivity | 22 electronics/count all Λ; 26 photons/count at 250 nm |
| Quantum efficiency | 90% peak; 65% at 250 nm |
| Optical Bench | |
| Design | f/4, Symmetrical crossed Czerny-Turner |
| Focal length | 101.6 mm input and output |
| Entrance aperture | 5, 10, 25, 50, 100, or 200 μm wide slits of fiber (no slit) |
| Spectroscopic | |
| Wavelength range | Grating dependent |
| Optical resolution | 0.14–7.7 nm FWHM |
| Signal-to-noise ratio | 1000:1 (at full signal) |
| Dynamic range | $7.5 \times 10^9$ (system), 25000:1 for a single acquisition |
| Integration time | 8 ms to 15 minutes |
| Stray light | < 0.08% at 600 nm; 0.4% at 436 nm |
| Corrected linearity | > 99% |

measure and evaluate the elastic light scattering of particle in this study. The 532 nm line of a solid-laser with output power 30 mW was used as the source of excitation. Before the laser beam was passed through the EDB, it was sent through a polarizer to maintain its polarization. A collimator with a focal length of 10 mm and the diameter of 5 mm was used to collimate the scattering of the levitated particle. The solid angle aperture of the collimator was about 5.7 degrees. The collimator was set up on the precision motorized rotation stage which calibrated with a stepping motor driver. As the stage was controlled by a stepping motor driver, the respective scattering angles could be verified. The integration time of each observation was 30 seconds. All measurements were made at room temperatures of 20–25°C.

## RESULTS AND DISCUSSION

The Figs. 2 and 4 demonstrated an experimental approach that provided insight into how particle size and refractive index affect the elastic scattering of PMMA and carbon particle. For comparison, numerical simulations based on the Lorenz-Mie theory were also displayed.

As demonstrated in Figs. 2(a), 2(b), and 2(c), the intensity of scattered light polarized perpendicular to the scatter plane was sensitive to scattering angle and particle diameter. Besides, as illustrated in Figs. 2(d), 2(e), and 2(f), the results showed the less oscillation in the forward scattering region that contributed by the parallel polarization of light. The results suggested that the larger particle contributes more oscillations and scattering intensity to the angular scattering curve (Ioannidou, 2005; Redmond *et al.*, 2010; Zhang and Rubini, 2011; Dlugach *et al.* 2012; Sorensen *et al.*, 2014).

In addition, the micro-structural morphology of the test particles was observed by Scanning Electron Microscope (SEM). At higher magnifications of 10000X, the structure and surface characteristic of PMMA particles could be clearly revealed. Fig. 3 showed SEM micrographs of PMMA particles with a diameter in about 5, 10, and 15 μm. As shown in Figs. 3(a), 3(b), and 3(c), most of the PMMA particles were spherical but some were concave and almost had a heavily wrinkled outer surface. The results demonstrated that the slightly deviations of backward scattering might be caused by the wrinkled surface characteristic of the particle (Li *et al.*, 2004; Yang *et al.*, 2007).

For a carbon particle, as displayed in Fig. 4, the intensity of scattered light either polarized perpendicular or polarized parallel to the scatter plane was insensitive to scattering angle but particle diameter in some scattering regions. In contrast, as illustrated in Figs. 4(d), 4(e), and 4(f), the results showed the a few oscillations in the forward scattering region that contributed by the parallel polarization of light. The refractive index influenced scattering (or extinction) in the small particle size region more than in the coarse particle size region (Bäumer *et al.*, 2008; Jung and Kim, 2008; Kostinski and Mongkolsittisilp, 2013).

The structure and surface characteristic of carbon particles was also observed by SEM at normal magnifications of 5000X. The Fig. 5 showed SEM micrographs of carbon particles with an aerodynamic diameter in about 5, 10, and 15 μm. As shown in Figs. 5(a), 5(b), and 5(c), most of the carbon particles were irregular, non-spherical and other small particles might agglomerate on the surface to effectively increase surface roughness.

Basing on the following equation, the aerodynamic diameter ($d_a$) could be translated into equivalent volume diameter (Hinds, 1999).

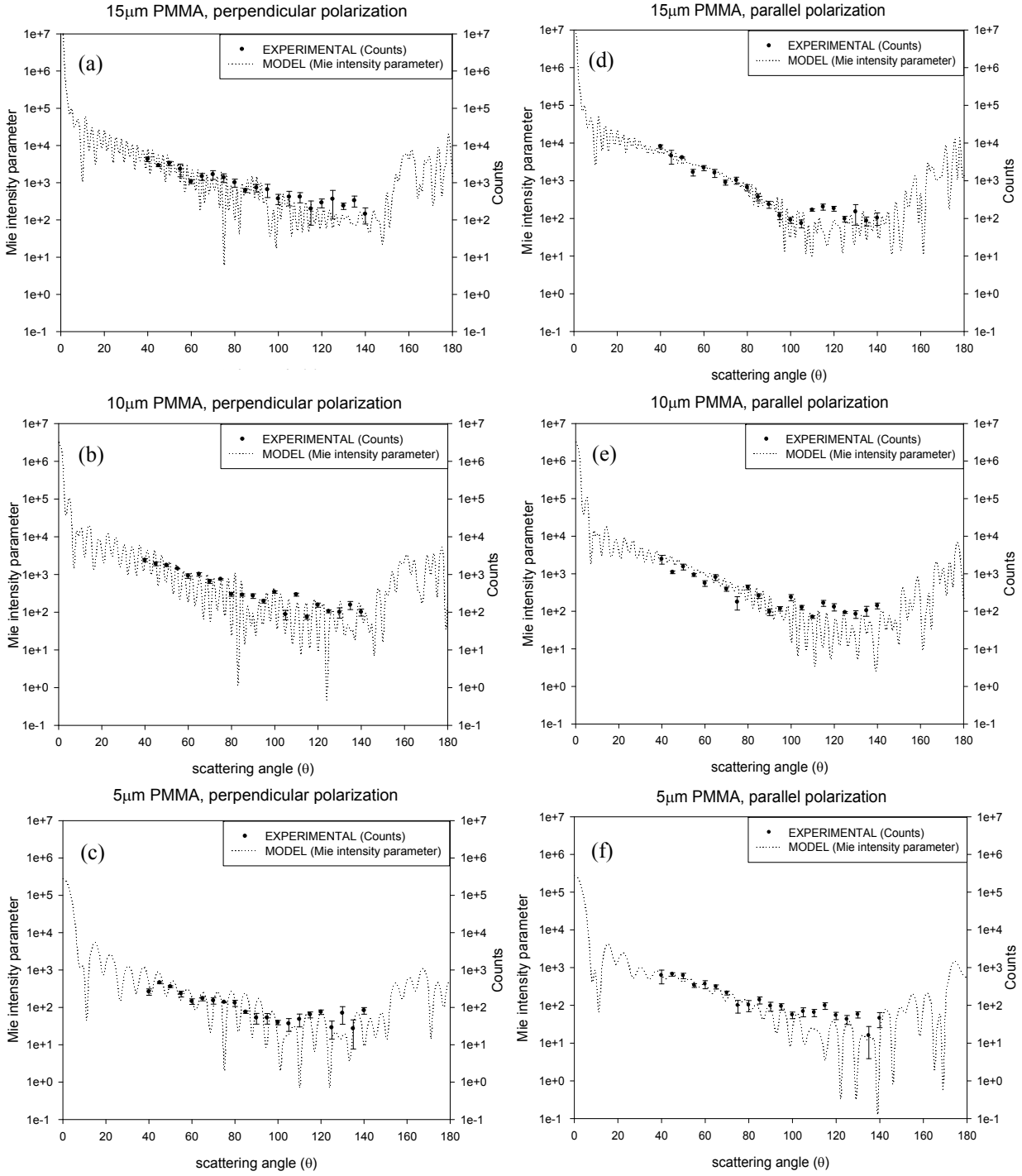


**Fig. 2.** The scattering intensity as a function of scattering angle for a PMMA particle.

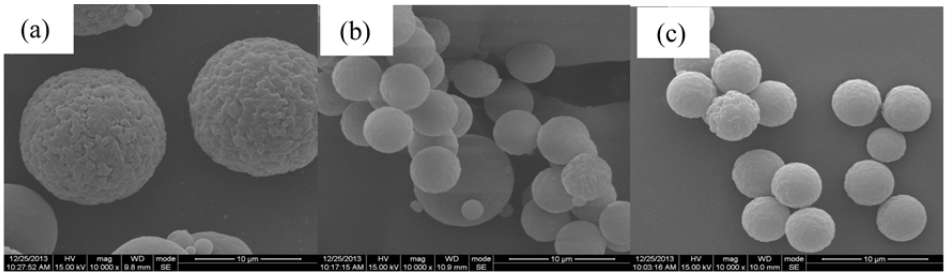


**Fig. 3.** The SEM micrograph of PMMA particles.

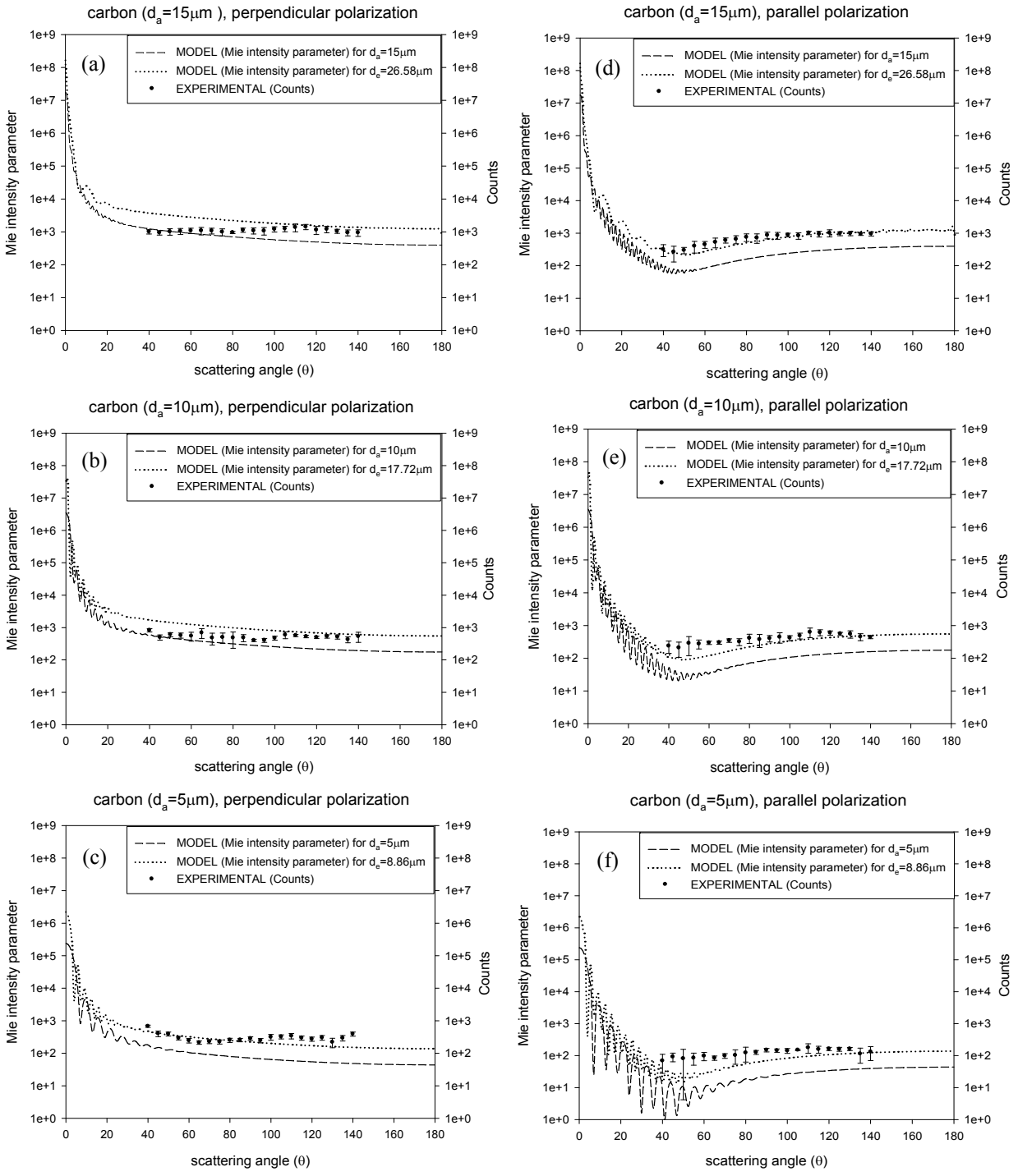


**Fig. 4.** The scattering intensity as a function of scattering angle for a carbon particle.

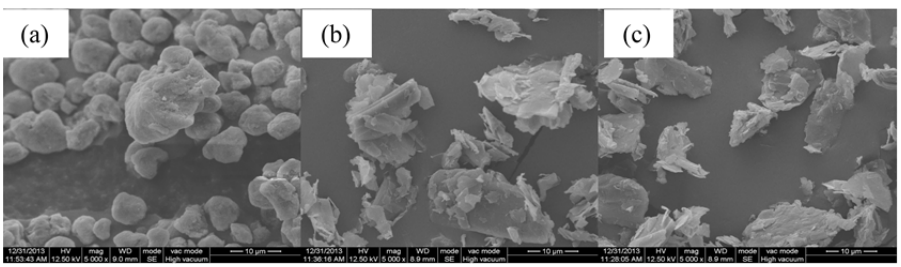


**Fig. 5.** The SEM micrograph of carbon particles.

$$d_a = d_e\sqrt{\frac{\rho_p}{\rho_0\chi}} \tag{9}$$

where $\rho_0$ was the standard particle density and $\rho_p$ was the carbon density, 433 kg m$^{-3}$ which provided from manufacturer. The $\chi$ was dynamic shape factor. Additionally, it was important to note that the simulation might result in significant deviations in the overall scattering because of using aerodynamic diameter to replace equivalent volume diameter ($d_e$). Although the aerodynamic diameter was widely applied in aerosol science and technology, the equivalent volume diameter might be involved in optical properties.

Consequently, it was interesting to note that the appearance of the varied backward scattering between numerical evaluations and experimental results because of the irregular structure or wrinkled surface characteristic of particle. Several theoretical and experimental studies also had shown that the non-spherical or irregular particle could lead to significant deviations in the scattering function calculated by the Lorenz-Mie theory, particularly at backward scattering directions (Curtis *et al.*, 2007; Aptowicz *et al.*, 2013).

According to the following equation, the initial value of the charge on a particle could be calculated (Hinds, 1999). Assuming there was no loss of the particle charge in the process which the particle diameter was increased with increasing relative humidity. By adjusting the DC voltage, the electrostatic force could be made to balance the force of gravity and the particle held stationary. At this moment,

$$neE = \frac{\rho_p \pi d^3 g}{6} \tag{10}$$

Correspondingly, by replacing the initial value of the particle charge as n, the variation of particle diameter could be determined in higher relative humidity. Hence, the variation of relative mass of the particle due to condensation or evaporation of water in response to the changes in ambient RH was determined by recording the $V_{dc}$ required to balance the weight of the particle. The specifications of parameter and refractive index were categorized in Table 3. The volume average and mass average refractive indices were separately calculated from the volumes and masses of the carbon and water.

As demonstrated in Figs. 6(a) and 6(b), the experimentally measured elastic scattering intensity was in good agreement of backward scattering but in the enhancement of forward scattering with numerical simulations. The experimental results also indicated the scattering intensity increased with the increasing of relative humidity. The trend of experimental results was similar with many studies (Yoon and Kim, 2006; Cheng *et al.*, 2008; Deng *et al.*, 2013; Liu *et al.*, 2013; Pilinis *et al.*, 2014).

Some studies also demonstrated that the scattering efficiency occurred an increasing behavior above 50% relative humidity and water uptake would not only change the refractive index but also particle size (Cheng *et al.*, 2008; Lyamani *et al.*, 2008; Li *et al.*, 2011). Besides, it was

**Table 3.** The specifications of parameter and reflective index.

| RH% | Dp | Total volume | Δvolume | volume fraction of water | volume fraction of carbon | mass fraction of water | mass fraction of carbon | refractive index (avg. by mass) | refractive index (avg. by vol.) |
|---|---|---|---|---|---|---|---|---|---|
| 30 | 1.772E-05 | 2.92E-15 | - | - | 1 | - | 1 | 2.00-i | 2.00-i |
| 50 | 1.959E-05 | 3.94E-15 | 1.023E-15 | 0.26 | 0.74 | 0.45 | 0.55 | 1.70–0.55i | 1.83–0.74i |
| 70 | 2.116E-05 | 4.96E-15 | 2.046E-15 | 0.41 | 0.59 | 0.62 | 0.38 | 1.59–0.38i | 1.72–0.59i |

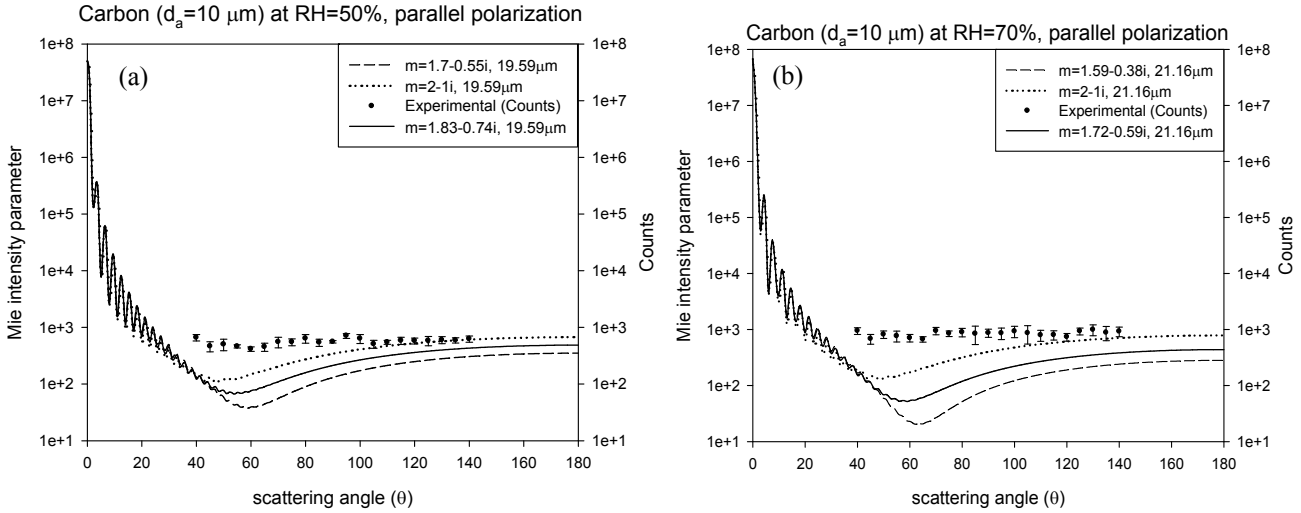


**Fig. 6.** The scattering intensity as a function of scattering angle for a carbon particle at relative humidity= 50 and 70%.

important to note that when using volume average method to estimate the effective refractive index of multicomponent or heterogeneous particle might cause some significant deviations between the theoretical and experimental result because of variations of the mixing state and the water distribution on the particle surface (Watson *et al.*, 2008; Deng *et al.*, 2013; Pilinis *et al.*, 2014).

Furthermore, the hygroscopic characteristics of particle were important to both direct and indirect forcing of global climate and atmospheric visibility reduction phenomena. The forward scattering of the ambient aerosols was especially affected by water uptake (Balis *et al.*, 2003; Gangl *et al.*, 2008; Liu *et al.*, 2008).

## CONCLUSIONS

This automatically electrodynamic balance system might be not only conducted a steady levitation of single particle but also provided an advantage measurement of light scattering. The experimental results presented that the measurements of light scattering were in approximate trend with numerical simulations basing on the Lorenz-Mie theory. Furthermore, simulation results also indicated that the scattering intensity might be underestimated in backward scattering directions.

For a light-scattering material, like PMMA, the scattering intensity of perpendicular polarization was sensitive to angle; furthermore, parallel polarization provided less oscillation in the forward scattering regions. In addition, the larger particle contributed more oscillations and higher intensity to the scattering curve.

For a light-absorbing material, like carbon, the scattering intensity of perpendicular and parallel polarization was insensitive to scattering angle but particle diameter. By contrast, parallel polarization provided a few oscillations in the forward scattering regions. Accordingly, the results showed that the simulation might result in significant deviations in the overall scattering while using aerodynamic diameter to replace equivalent volume diameter. Besides, the results also showed that the scattering intensity increased with the increasing of relative humidity.

According to the micro-structural morphology, the results showed that the appearance of backward scattering was varied with the irregular structure or wrinkled surface characteristic. Moreover, the results suggested that while using the weighted average method to estimate the refractive index of heterogeneous particle might cause some significant deviations of light scattering between measuring and modeling.

## REFERENCES

Aptowicz, K.B., Pan, Y.L., Martin, S.D., Fernandez, E., Chang, R.K. and Pinnick, R.G. (2013). Decomposition of atmospheric aerosol phase function by particle size and asphericity from measurements of single particle optical scattering patterns. *J. Quant. Spectrosc. Radiat. Transfer* 131: 13–23.

Bagheri, G.H., Bonadonna, C., Manzella, I. and Vonlanthen, P. (2015). On the characterization of size and shape of irregular particles. *Powder Technol.* 270: 141–153.

Balis, D.S., Amiridis, V., Zerefos, C., Gerasopoulos, E., Andreae, M., Zanis, P., Kazantzidis, A., Kazadzis, S. and Papayannis, A. (2003). Raman lidar and sunphotometric measurements of aerosol optical properties over Thessaloniki, Greece during a biomass burning episode. *Atmos. Environ.* 37: 4529–4538.

Bäumer, D., Vogel, B., Versick, S, Rinke, R., Möhler, O. and Schnaiter, M. (2008). Relationship of visibility, aerosol optical thickness and aerosol size distribution in an ageing air mass over South-West Germany. *Atmos. Environ.* 42: 989–998.

Briard, P., Wang, J.J. and Han, Y.P. (2016). Shaped beam scattering by an aggregate of particles using generalized Lorenz-Mie theory. *Opt. Commun.* 365: 186–193.

Cariou, J.M., Dugas, J., Martin, L. and Michel, P. (1986). Refractive-index variations with temperature of PMMA and polycarbonate. *Appl. Opt.* 25: 334–336.

Chan, M.N. and Chan, C.K. (2007). Mass transfer effects

on the hygroscopic growth of ammonium sulfate particles with a water-insoluble coating. *Atmos. Environ.* 41: 4423–4433.

Chang, H. and Biswas, P. (1992). In situ light scattering dissymmetry measurements of the evolution of the aerosol size distribution in flames. *J. Colloid Interface Sci.* 153: 157–166.

Charlson, R.J., Schwartz, S.E., Hales, J.M., Cess, R.D., Coakley, J.A., Hansen, J.E. and Hofmann, D.J. (1992). Climate forcing by anthropogenic aerosols. *Science* 255: 423–430.

Chen, L.Y., Chou, M.C., Hwang, L.K., Lin, W.Y., Chen, C.C. and Jeng, F.T. (2000). Aerosol scattering coefficients at different humidities. *J. Aerosol Sci.* 31: S983–S984.

Cheng, Y.F., Wiedensohler, A., Eichler, H., Su, H., Gnauk, T., Brüggemann, E., Herrmann, H., Heintzenberg, J., Slanina, J., Tuch, T., Hu, M. and Zhang, Y.H. (2008). Aerosol optical properties and related chemical apportionment at Xinken in Pearl River Delta of China. *Atmos. Environ.* 42: 6351–6372.

Curtis, D.B., Aycibin, M., Young, M.A., Grassian, V.H. and Kleiber, P.D. (2007). Simultaneous measurement of light-scattering properties and particle size distribution for aerosols: Application to ammonium sulfate and quartz aerosol particles. *Atmos. Environ.* 41: 4748–4758.

Dave, J.V. (1968). Subroutine for Computing the Parameters of the Electromagnetic Radiation Scattered by a Sphere. IBM Science Center Report No. 320–3237.

Davis, E.J. (1985). Electrodynamic balance stability characteristics and applications to the study of aerosolloidal particles. *Langmuir* 1: 379–387.

Davis, E.J. (1997). A history of single aerosol particle levitation. *Aerosol Sci. Technol.* 26: 212–254.

Davis, E.J. and Bridges, M.A. (1994). The Rayleigh limit of charge revisited: Light scattering from exploding droplets. *J. Aerosol Sci.* 25: 1179–1199.

Davis, E.J. and Schweiger, G. (2002). *The Airborne Microparticle: Its Physics, Chemistry, Optics, and Transport Phenomena*. Springer, Berlin.

Davies, J.F., Haddrell, A.E. and Reid, J.P. (2012). Time-resolved measurements of the evaporation of volatile components from single aerosol droplets. *Aerosol Sci. Technol.* 46: 666–677.

De Leeuw, G. and Lamberts, C.W. (1987). Influence of refractive index and particle size interval on Mie calculated backscatter and extinction. *J. Aerosol Sci.* 18: 131–138

Deng, J., Du, K., Wang, W. and Rood, M.J. (2013). Closure study on measured and modeled optical properties for dry and hydrated laboratory inorganic aerosols with mixtures of dicarboxylic acids. *Atmos. Environ.* 81: 177–187.

Dlugach, J.M., Mishchenko, M.I. and Mackowski, D.W. (2012). Scattering and absorption properties of polydisperse wavelength-sized particles covered with much smaller grains. *J. Quant. Spectrosc. Radiat. Transfer* 113: 2351–2355.

Dlugach, J.M. and Mishchenko, M.I. (2014). Effects of nonsphericity on the behavior of Lorenz-Mie resonances in scattering characteristics of liquid-cloud droplets. *J. Quant. Spectrosc. Radiat. Transfer* 146: 227–234.

Friedlander, S.K. (2000). *Smoke, Dust, and Haze: Fundamentals of Aerosol Dynamics*. Oxford University Press, Oxford, New York.

Fukushima, S., Zhang, D., Shibata, T., Katagiri, S. and Hayasaka, T. (2016). Dependence of backscattering coefficients of atmospheric particles on their concentration and constitution under dry and humid conditions at Southwestern Japanese coast in Spring. *Aerosol Air Qual. Res.* 16: 1294–1301.

Gangl, M., Kocifaj, M., Videen, G. and Horvath, H. (2008). Light absorption by coated nano-sized carbonaceous particles. *Atmos. Environ.* 42: 2571–2581.

Gatherer, R.D.B., Sayer, R.M. and Reid, J.P. (2002). An optical method for determining size distributions of water droplets. *Chem. Phys. Lett.* 366: 34–41.

Greengard, L., Hagstrom, T. and Jiang, S. (2015). Extension of the Lorenz-Mie-Debye method for electromagnetic scattering to the time-domain. *J. Comput. Phys.* 299: 98–105.

Haddrell, A.E., Davies, J.F., Miles, R.E.H., Reid, J.P., Dailey, L.A. and Murnane, D. (2014). Dynamics of aerosol size during inhalation: Hygroscopic growth of commercial nebulizer formulations. *Int. J. Pharm.* 463: 50–61.

Haddrell, A.E., Hargreaves, G., Davies, J.F. and Reid, J.P. (2013). Control over hygroscopic growth of saline aqueous using Pluronic polymer additives. *Int. J. Pharm.* 443: 183–192.

Haddrell, A.E., Feng, X., Nassar, R., Bogan, M.J. and Agnes, G.R. (2005). Off-line LDI-TOF-MS monitoring of simultaneous inorganic and organic reactions on particles levitated in a laboratory environment. *J. Aerosol Sci.* 36: 521–533.

Hajihashemi, M.R. and Jiang, H. (2013). Gaussian random ellipsoid geometry-based morphometric recovery of irregular particles using light scattering spectroscopy. *J. Quant. Spectrosc. Radiat. Transfer* 118: 86–95.

Han, L., Han, Y.P., Cui, Z.W. and Wang, J.J. (2014). Expansion of a zero-order Bessel beam in spheroidal coordinates by generalized Lorenz-Mie theory. *J. Quant. Spectrosc. Radiat. Transfer* 147: 279–287.

Hinds, W.C. (1999). *Aerosol Technology - Properties, Behavior, and Measurement of Airborne Particles*. John-Wiley & Sons, New York.

Hopkins, R.J., Symes, R., Sayer, R.M. and Reid, J.P. (2003). Determination of the size and composition multicomponent ethanol/water droplets by cavity-enhanced Raman scattering. *Chem. Phys. Lett.* 380: 665–672.

Ioannidou, M.P. (2005). Study of atmospheric visibility pertaining to soot scavenging by sulfate droplets. *J. Quant. Spectrosc. Radiat. Transfer* 96: 473–485.

IPCC (2013). *Summary for Policymakers. In: Climate Change 2013: The Physical Science Basis. Contribution of Working Group I to the Fifth Assessment Report of the Intergovernmental Panel on Climate Change* Stocker, T.F., Qin, D., Plattner, G.K., Tignor, M., Allen, S.K., Boschung, J., Nauels, A., Xia, Y., Bex, V. and Midgley, P.M. (Eds.), Cambridge University Press, Cambridge, United Kingdom and New York, NY, USA.

Jarzembski, M.A. and Tankosic, D.V. (2005). Discharge of negatively charged micrometer size particles in an electrodynamic balance due to radioactivity. *J. Aerosol Sci.* 36: 1023–1035.

Jung, C.H. and Kim, Y.P. (2008). Theoretical study on the change of the particle extinction coefficient during the aerosol dynamic processes. *J. Aerosol Sci.* 39: 904–916.

Kawamoto, H. (2009). Manipulation of single particles by utilizing electrostatic force. *J. Electrostat.* 67: 850–861.

Kelly, J.T., Wexler, A.S., Chan, C.K. and Chan, M.N. (2008). Aerosol thermodynamics of potassium salts, double salts, and water content near the eutectic. *Atmos. Environ.* 42: 3717–3728.

Kiehl, J.T. and Briegleb, B.P. (1993). The relative roles of sulfate aerosols and greenhouse gases in clime forcing. *Science* 260: 311–314.

Kim, K.W. (2015). Optical properties of size-resolved aerosol chemistry and visibility variation observed in the urban site of Seoul, Korea. *Aerosol Air Qual. Res.* 15: 271–283.

Knox, K.J., Symes, R. and Reid, J.P. (2010). Fluorescence spectroscopy and signaling from optically-tweezed aerosol droplets. *Chem. Phys. Lett.* 487: 165–170.

Kostinski, A.B. and Mongkolsitsilp, A. (2013). Minimum principles in electronmagnetic scattering by small aspherical particles. *J. Quant. Spectrosc. Radiat. Transfer* 131: 194–201.

Lee, C.T. and Hsu, W.C. (1999). Effects of local pollution and environmental humidity on aerosol size spectra and light-scattering coefficients in southern Taiwan. *Environ. Int*. 25: 433–441.

Li, C.H., Kattawar, G.W. and Yang, P. (2004). Effects of surface roughness on light scattering by small particles. *J. Quant. Spectrosc. Radiat. Transfer* 89: 123–131.

Li, X., Xie, L. and Zheng, X. (2012). The comparison between the Mie theory and the Rayleigh approximation to calculate the EM scattering by partially charged sand. *J. Quant. Spectrosc. Radiat. Transfer* 113: 251–258.

Li, Y., Ezell, M.J. and Finlayson-Pitts, B.J. (2011). The impact of organic coatings on light scattering by sodium chloride particles. *Atmos. Environ.* 45: 4123–4132.

Lin, W.Y., Huang, L.K., Chen, L.Y., Chen, C.C. and Jeng, F.T. (2000). Opacity of monodisperse aerosol in down – scale transmissometer. *J. Aerosol Sci.* 31: S785–S786.

Lin, Y.C., Cheng, M.T., Chio, C.P. and Kuo, C.Y. (2009). Carbonaceous Aerosol Measurements at Coastal, Urban, and Inland Sites in Central Taiwan. *Environ. Forensics* 10: 7–17.

Lin, Y.C., Cheng, M.T., Lin, W.H., Lan, Y.Y. and Tsuang, B.J. (2010). Causes of the elevated nitrate aerosol levels during episodic days in Taichung urban area, Taiwan. *Atmos. Environ.* 44: 1632–1640.

Liu, L. and Mishchenko, M.I. (2007). Scattering and radiative properties of complex soot and soot-containing aggregate particles. *J. Quant. Spectrosc. Radiat. Transfer* 106: 262–273.

Liu, X., Cheng, Y., Zhang, Y., Jung, J., Sugimoto, N., Chang, S.Y., Kim, Y.J., Fan, S. and Zeng, L. (2008). Influences of relative humidity and particle chemical composition on aerosol scattering properties during the 2006 PRD campaign. *Atmos. Environ.* 42: 1525–1536.

Liu, X., Gu, J., Li, Y., Cheng, Y., Qu, Y., Han, T., Wang, J., Tian, H., Chen, J. and Zhang, Y. (2013). Increase of aerosol scattering by hygroscopic growth: Observation, modeling, and implications on visibility. *Atmos. Res.* 132–133: 91–101.

Lyamani, H., Olmo, F.J. and Alados-Arboledas, L. (2008). Light scattering and absorption properties of aerosol particles in the urban environment of Granada, Spain. *Atmos. Environ.* 42: 2630–2642.

Ma, L. (2007). Measurement of aerosol size distribution function using Mie scattering – Mathematical considerations. *J. Aerosol Sci.* 38: 1150–1162.

Millikan, R.A. (1935). *Electrons (+ and -), Protons, Photons, Neutrons, and Cosmic Rays*. University of Chicago Press, Chicago.

Milstein, A.B. and Richardson, J.M. (2015). Comparison of models and measurements of angle-resolved scatter from irregular aerosols. *J. Quant. Spectrosc. Radiat. Transfer* 151: 110–122.

Mitchem, L., Hopkins, J., Buajarern, J., Ward, A.D. and Reid, J.P. (2006). Comparative measurements of aerosol droplet growth. *Chem. Phys. Lett.* 432: 362–366.

Molnár, A., Bécsi, Z., Imre, K., Gácser, V. and Ferenczi, Z. (2016). Characterization of background aerosol properties during a wintertime smog episode. *Aerosol Air Qual. Res.* 16: 1793–1804.

Moreno, F., Vilaplana, R., Muñoz, O., Molina, A. and Guirado, D. (2006). The scattering matrix for size distribution of irregular particles: An application to an olivine sample. *J. Quant. Spectrosc. Radiat. Transfer* 100: 277–287.

Muñoz, O., Moreno, F., Guirado, D., Ramos, J.L., López, A., Girela, F., Jerónimo, J.M., Costillo, L.P. and Bustamante, I. (2010). Experimental determination of scattering matrices of dust particles at visible wavelengths: The IAA light scattering apparatus. *J. Quant. Spectrosc. Radiat. Transfer* 111: 187–196.

Muñoz, O. and Hovenier, J.W. (2011). Laboratory measurements of single light scattering by ensembles of randomly oriented small irregular particles in air. A review. *J. Quant. Spectrosc. Radiat. Transfer* 112: 1646–1657.

Nakajima, Y. (2006). A measuring system for the time variation of size and charge of a single spherical particle and its applications. *Chem. Eng. Sci.* 61: 2212–2229.

Peng, C.G. and Chan, C.K. (2001). The water cycles of water-soluble organic salts of atmospheric importance. *Atmos. Environ.* 35: 1183–1192.

Petrov, D., Shkuratov, Y. and Videen, G. (2011). Electromagnetic wave scattering from particles of arbitrary shapes. *J. Quant. Spectrosc. Radiat. Transfer* 112: 1636–1645.

Pilinis, C., Charalampidis, P. E., Mihalopoulos, N. and Pandis, S.N. (2014). Contribution of particulate water to the measured aerosol optical properties of aged aerosol. *Atmos. Environ.* 82: 144–153.

Pu, W., Wang, X., Zhang, X., Ren, Y., Shi, J.S., Bi, J.R.,

and Zhang, B.D. (2015). Size distribution and optical properties of particulate matter ($PM_{10}$) and black carbon (BC) during dust storms and local air pollution events across a loess plateau site. *Aerosol Air Qual. Res.* 15: 2212–2224.

Redmond, H.E., Dial, K.D. and Thompson, J.E. (2010). Light scattering and absorption by wind blown dust: Theory, measurement, and recent data. *Aeolian Res.* 2: 5–26.

Reid, J.P. (2009). Particle levitation and laboratory scattering. *J. Quant. Spectrosc. Radiat. Transfer* 110: 1293–1306.

Richardson, C.B., Pigg, A.L. and Hightower, R.L. (1989). On the stability limit of charged droplet. *Proc. R. Soc. London, Ser. A* 422: 319–328.

Shah, G.A. (1992). Geometrical Optics and Diffraction vis-à-vis Mie theory of scattering of electromagnetic radiation by a sphere. *Astrophys. Space Sci.* 193: 317–328.

Sorensen, C.M., Zubko, E., Heinon, W.R. and Chakrabarti, A. (2014). Q–space analysis of scattering by small irregular particles. *J. Quant. Spectrosc. Radiat. Transfer* 133: 99–105.

Symes, R., Meresman, H., Sayer, R.M. and Reid, J.P. (2006). A quantitative demonstration of the enhancement of cavity enhanced Raman scattering by broad band external laser seeding. *Chem. Phys. Lett.* 419: 545–549.

Tsai, C.S. (2007). *Development of Single Particle Automatic Suspension and Measurement System*. Master thesis, National Taipei University of Technology, Taipei, Taiwan.

Van de Hulst, H.C. (1981). *Light Scattering by Small Particles*. Dover, New York.

Volten, H., De Haan, J.F., Vassen, W., Lumme, K. and Hovenier, J.W. (1996). Experimental determination of polarized light scattering by irregular particles. *J. Aerosol Sci.* 27: S527–S528.

Wang, Y., Chakrabarti, A. and Sorensen, C.M. (2015). A light- scattering study of the scattering matrix elements of Arizona Road Dust. *J. Quant. Spectrosc. Radiat. Transfer* 163: 72–79.

Watson, J.G., Chow, J.C. and Chen, L.W.A. (2005). Summary of organic and elemental carbon/black carbon analysis methods and intercomparisons. *Aerosol Air Qual. Res.* 5: 65–102.

Watson, J.G., Chow, J.C., Lowenthal, D.H. and Magliano, K.L. (2008). Estimating aerosol light scattering at the Fresno Supersite, *Atmos. Environ.* 42: 1186–1196.

Wills, J.B., Knox, K.J. and Reid, J.P. (2009). Optical control and charaterisation of aerosol. *Chem. Phys. Lett.* 481: 153–165.

Wolfram, H. and Thomas, W. (2012). *The Mie Theory: Basics and Applications*. Springer Series in Optical Sciences, Vol. 169.

Wu, Y., Zhang, R., Pu, Y., Zhang, L., Ho, K.F, and Fu, C. (2012). Aerosol optical properties observed at a semi-arid rural site in Northeastern China. *Aerosol Air Qual. Res.* 12: 503–514.

Yang, M.L., Wu, Y.Q., Sheng, X.Q. and Ren, K.F. (2015). Comparison of scattering diagrams of large non-spherical particles calculated by VCRM and MLFMA. *J. Quant. Spectrosc. Radiat. Transfer* 162: 143–153.

Yang, P., Feng, Q., Hong, G., Kattawar, G.W., Wiscombe, W.J., Mishchenko, M.I., Dubovik, O., Laszlo, I. and Sokolik, I.N. (2007). Modeling of the scattering and radiative properties of nonspherical dust-like aerosols. *J. Aerosol Sci.* 38: 995–1014.

Yoon, S.C. and Kim, J. (2006). Influences of relative humidity on aerosol optical properties and aerosol radiative forcing during ACE-Asia. *Atmos. Environ.* 40: 4328–4338.

Zaitone, B.A.A. and Tropea, C. (2011). Evaporation of pure liquid droplets: Comparison of droplet evaporation in an acoustic field versus glass-filament. *Chem. Eng. Sci.* 66: 3914–3921.

Zhang, Q. and Rubini, P.A. (2011). Modelling of light extinction by soot particles. *Fire Saf. J.* 46: 96–103.

Zubko, E., Muinonen, K., Muñoz, O., Nousiainen, T., Shkuratov, Y., Sun, W. and Videen, G. (2013). Light scattering by irregular particles: Comparison of model agglomerate debris particles with laboratory samples. *J. Quant. Spectrosc. Radiat. Transfer* 131: 175–187.

*Received for review, November 13, 2016*
*Revised, February 19, 2017*
*Accepted, March 21, 2017*